Available online at www.sciencedirect.com
ScienceDirect
Surface & Coatings Technology 202 (2008) 3988–3996
SURFACE & COATINGS TECHNOLOGY
www.elsevier.com/locate/surfcoat

Properties of SiC-reinforced aluminum alloy coatings produced by the cold gas dynamic spraying process

E. Sansoucy [a], P. Marcoux [b], L. Ajdelsztajn [a], B. Jodoin [a,*]

[a] Department of Mechanical Engineering, University of Ottawa, Ottawa, Ontario, Canada
[b] Vac Aero International Inc., Boucherville, Québec, Canada

Received 11 October 2007; accepted in revised form 12 February 2008
Available online 29 February 2008

Abstract

SiC-reinforced Al–12Si alloy coatings were produced using the Cold Gas Dynamic Spraying process. Blends of several compositional variations of Al–12Si and SiC particles were created and subsequently sprayed. The microstructural features of the resulting coatings are examined and the mechanical properties, in particular the adhesion strength and the hardness, of the composite coatings are reported. The results show that, depending on the initial SiC volume fraction of the blend, between 50% and 33% of the SiC in the feedstock powder was retained in the coatings. The adhesion strength of the coatings to their substrates was found to slightly decrease with increasing SiC content while the inclusion of SiC particles within the Al–12Si matrix improved significantly the hardness of the coating.

Keywords: Cold Gas Dynamic Spraying; Metal matrix composite(MMC); Aluminum alloy; SiC reinforcement

1. Introduction

Metal matrix composites (MMCs) constitute a class of materials that have made a major industrial impact in fields as diverse as aerospace, automotives, and electronics. These materials can be tailored to yield superior properties by incorporating a controlled amount of reinforcement within a metal matrix. Alloys reinforced with particulate ceramics can offer property enhancements such as increased hardness, improved wear resistance, better thermal stability, and superior yield strength [1,2]. Among the various matrix materials available, aluminum and its alloys are widely used in the fabrication of MMCs. This is mainly due to the low density, high strength, and good corrosion resistance of aluminum alloys. These alloys are also cheaper than other low density alloys such as magnesium or titanium and can be produced by various processing techniques, such as extrusion, forging, casting, and powder metallurgy.

In particular, it has been reported that the addition of relatively inexpensive silicon carbide (SiC) particles to an aluminum alloy matrix has resulted in an increase in the strength [3], elastic modulus [3], and wear resistance [4]. These composites have a slightly inferior corrosion resistance when compared to the aluminum alloy matrix itself. The presence of SiC particles embedded in an aluminum matrix represents discontinuities and oxidation has been shown to occur at the interface of the reinforcement and the aluminum alloy matrix [5].

Such MMCs have emerged as an important class of high-performance structural elements in the automotive and space industries [6,7]. Major fabrication methods of these aluminum–SiC composites include casting, extrusion, spray deposition, and powder metallurgy [8]. It has been shown that the presence of defects such as porosity, shrinkage, oxide inclusions, clustering of silicon carbide particles, and degradation of the reinforcement phase significantly influence the bulk and the coating properties [3,8]. In addition, the low-temperature ductility and poor toughness generally encountered are drawbacks that limit the performance and applications of such composites. Al–SiC composite coatings produced by plasma spray exhibit properties characteristic of bulk composites such as high wear resistance [9].

* Corresponding author. 161 Louis Pasteur, Room A205, Ottawa, Ontario, Canada K1N 6N5. Tel.: +1 613 562 5800x6280; fax: +1 613 562 5177.
E-mail address: jodoin@genie.uottawa.ca (B. Jodoin).

0257-8972/$ - see front matter © 2008 Elsevier B.V. All rights reserved.
doi:10.1016/j.surfcoat.2008.02.017

High quality SiC-reinforced composite coatings have also been obtained using low velocity oxygen-fuel spraying [10]. As a result, these coatings are a viable method to improve the surface properties of components without producing any significant change in their ductility.

The SiC particle distribution and volume fraction in plasma sprayed composite coatings depend on the quality of the feedstock powder which is being used for spraying. In feedstock powders prepared by blending SiC with aluminum alloy particles, SiC particles are preferentially lost compared to the aluminum alloy particles [10–13]. The large difference in melting temperatures between the SiC and the aluminum alloy and poor wettability of SiC by aluminum explain this behavior [11–13]. During the plasma spraying process, aluminum particles are melted by the plasma gas and solidify upon impact on the substrate. However, the SiC particles remain in their solid state and are entrapped in the sprayed material or rebound off the surface of the deposit. Excess amount of SiC particles must then be added to the feedstock to compensate for the SiC lost during the spraying process. It was reported that increasing the SiC content in the feedstock powder beyond some value does not augment the SiC volume fraction in the coating [12,13]. This is attributed to the fact that less liquid aluminum is available, in proportion, to retain the SiC particles and to fill the voids in the coating. Plasma spraying of Al–SiC composite powders prepared by the mechanical alloying process has been found to produce coatings with uniformly distributed and fine reinforcements within an aluminum matrix [9,11,14]. In the mechanical alloying of composite powders, the particles of each constituent are added in a rotating ball mill and are continuously grinded. The repeated fracturing reduces the particles to a smaller size and cold welding produces agglomerations of aluminum particles with fragments of SiC [9,11,14]. The SiC particulates are then well incorporated and homogeneously dispersed within the composite powder which improves the wettability of SiC by aluminum and augment the fraction of SiC entrapped in the coatings [15].

The Cold Gas Dynamic Spraying (CGDS) process is an emerging thermal spray coating technology that can produce conventional [16–18], nanocrystalline [19–21], and amorphous coatings [22,23]. In this process, the powder particles are not in a softened, semi-molten, or molten state but it is believed that they remain in their solid state throughout the deposition process [17,24]. Fine powder particles are injected in a supersonic gas flow and accelerated above a critical velocity. Upon impact on the substrate, the particles deform plastically and bond to the substrate to form a coating [17,24]. The process is also capable of depositing a wide variety of aluminum alloy [25–27] and composite coatings [25,28–32].

Few studies have looked at the characteristics of SiC-reinforced aluminum alloy coatings produced by the CGDS. Previous studies have shown that deposits of hard materials such as SiC and Al_2O_3 incorporated in a ductile aluminum matrix can be successfully produced by the CGDS process [30]. It was reported that the thickness of the Al–SiC composite film could reach 50 μm when spraying on silicone substrates [30]. It has also been shown that changing the content of SiC particulates within an aluminum matrix produced predictable changes in the thermal properties such as the thermal conductivity and the coefficient of thermal expansion [28]. Composite coatings using an aluminum matrix with reinforcing particles of diamond, tungsten, silicon carbide, aluminum nitride or boron carbide have also been produced by CGDS [29,32].

Despite these early studies, the effects of SiC particles on the microstructure and the mechanical properties of aluminum matrix composite coatings produced by CGDS have yet to be examined. The objectives of this study are to develop and evaluate the properties of Al–12Si alloy coatings reinforced with dispersed SiC particles using the CGDS process. The Al–12Si alloy was chosen because it is a well known casting alloy used in the automotive and aerospace engineering sectors. Aluminum–silicon alloys possess a low thermal expansion coefficient, good corrosion resistance, and improved mechanical properties at a wide range of temperatures. This paper examines the effects of the ceramic particulate content and size in the feedstock powder on the coatings' microstructural features, adhesion, and hardness.

2. Experimental procedures

2.1. Powder preparation

The materials used in this study comprised of commercially available aluminum Al–12Si powder (Al-111, Praxair Surface Technologies, Indianapolis, IN, USA) and a reinforcement

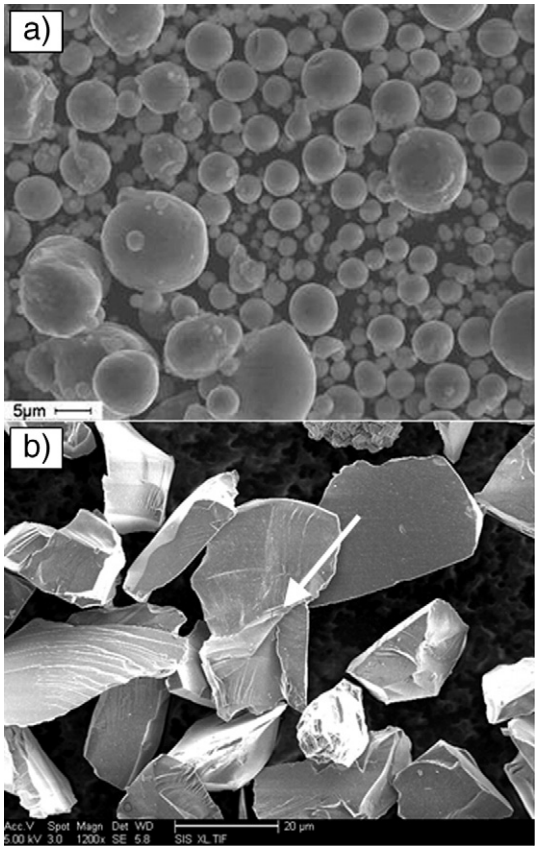

Fig. 1. Morphology of a) the Al–12Si and b) the SiC powders particles (the arrow points to a crack in a SiC particle).

phase of particulate SiC (Sika, Arendal Smelteverk, Norway). The aluminum alloy, produced by atomization, was composed of particles ranging between 5 to 45 μm in diameter. As shown in Fig. 1a), these particles have a spherical morphology. The morphology of the SiC particles is angular with sharp edges as a result of the crushing and grinding of SiC lumps that occur during their fabrication method (Fig. 1b)). A close examination of the SiC particle in the center of Fig. 1b) reveals a crack, as pointed out by the arrow. It was found that some SiC feedstock particles already contained cracks prior to spraying. Even though the SiC particles are slightly denser than the Al–12Si particles (3.2 g/cm^3 and 2.7 g/cm^3 for SiC and Al–12Si, respectively), both are expected to reach similar velocities prior to impact on the substrate as irregular shaped particles have been shown to experience larger drag coefficients than spherical particles [26,33]. The reinforcement particles were sieved below 25, 32, and 38 μm to have SiC particles with a size comparable to the Al–12Si particles. The SiC particles below 32 μm were mixed to the matrix alloy powder to create powder feedstock blends containing 20, 30, 40, and 60% volume of SiC. The SiC particles below 25 μm and 38 μm were combined to Al–12Si particles to produce blends with 20% volume of SiC in order to study the effect of the reinforcement particle size on the coating formation process and coating properties. The powder feedstock mixtures used for this study are summarized in Table 1.

2.2. Coating preparation

The SiC-reinforced aluminum alloy coatings were produced using the CGDS coating system developed at the University of Ottawa Cold Spray Laboratory. The system includes a spray chamber, a spray gun, a propellant gas heater, and a commercial powder feeder (Model 1264, Praxair Surface Technologies, Concord, NH, USA). The spray gun consists of a converging–diverging nozzle with an exit diameter of 7.3 mm. For the present work, helium was used as propellant gas at a gas stagnation pressure and temperature of 1.7 MPa and 360 °C, respectively. The coatings were produced on grit-blasted aluminum 6061-T6 substrates at a stand-off distance of 10 mm. A two-axis displacement system moved the substrate along a plane perpendicular to the spray gun axis. The substrates were grit-blasted using ebony (ferrosilicate) beads (20-grit) at a blasting pressure of 400 kPa (60 psi) and at a 45° blasting angle. No other surface treatment was applied to the substrate prior to spraying. The coatings were produced from a single passage of the substrate in front of the spray gun and at a powder feed rate of 2 g/min.

Table 1
Description of the mixed feedstock powders

Mixed feedstock powders	SiC (% vol.)	SiC size (μm)
Al–12Si+20%SiC (<25)	20	<25
Al–12Si+20%SiC (<32)	20	<32
Al–12Si+30%SiC (<32)	30	<32
Al–12Si+40%SiC (<32)	40	<32
Al–12Si+60%SiC (<32)	60	<32
Al–12Si+20%SiC (<38)	20	<38

2.3. Coating characterization

The coatings samples were sectioned and prepared for scanning electron microscopy (SEM), following standard metallographic techniques. Secondary electron and backscattered electron images of the coatings' cross-sections were used to evaluate the microstructural features such as the porosity and the volume fraction of the SiC phase. These were obtained using the Clemex image analysis software [34]. A quantitative separation of the coating's structural elements was performed based on the grey level distribution of the SEM images. The porosity (black contrast) and the SiC particles (deep grey contrast) could be distinguished by setting grey scale threshold cutoff points. The percent areas of the marked regions for porosity and for the SiC particles could then be measured independently.

Vickers microhardness tests were performed on the cross-section of the deposits using a 300 gf load and a dwell time of 10 s using a Duramin-1 microhardness tester (Struers Inc., Cleveland, OH, USA). The reported values are the average of 10 indentations for each sample.

Bond strength evaluations were conducted using the ASTM Standard C 633-01 [35]. Coatings were produced on grit-blasted standard test samples having a 25.4 mm diameter and an overall length of 38.1 mm. Several passes at a 50% overlap were carried out to cover the entire surface of the sample. The top portion of the coating was then machined flat and glued to an uncoated test sample. An adhesive (Master Bond EP-15, Hackensack, NJ, USA) was used for bonding the test specimens. The arrangement was then cured at 170 °C for 90 min in a V block device to ensure a proper alignment. Before testing the coatings, the bonding agent was tested separately on four uncoated test samples, and failed at 82±10 MPa, which conforms to the product specifications. The average adhesion strength was determined based on three test samples.

2.4. Particle velocity measurements

Particle velocities were measured with a laser in-flight diagnostic system, a Cold Spray Meter (CSM) (Tecnar Automation Ltd., St-Bruno, Québec, Canada). While a continuous laser illuminates a measurement volume, a dual-slit photomask captures the signal generated by individual particles passing in front of the sensor. The signal from the photosensor is then amplified, filtered, and analyzed. In-flight diagnostic of each individual particle that crosses the measurement volume is performed by determining the time between two peaks of the particle signal. Particle velocities are then obtained by dividing the time distance between the two-slits by their time of flight [36]. In this study, the velocity measurements were taken at a point 10 mm from the spray gun exit. In order to avoid particle build-ups and rebounds that could obstruct the sensor field of view, the particle velocity

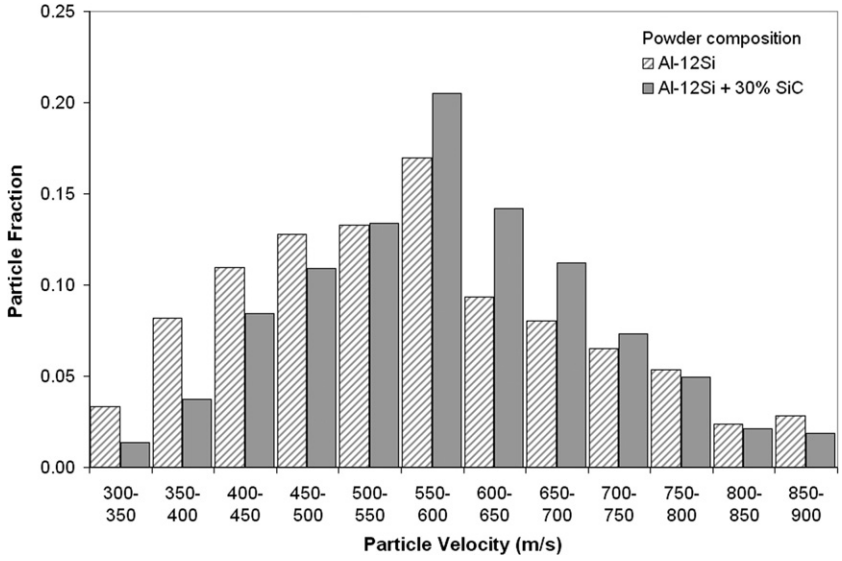

Fig. 2. Measured particle velocity distributions for the Al–12Si powder and the mixture with 30% volume of SiC particles below 32 μm.

measurements were performed without a substrate at the exit of the spray gun.

3. Results and discussion

3.1. Particle velocity measurements

Particle velocity measurements were first undertaken to obtain the in-flight particle velocity distributions of pure and mixed feedstock powders. The particle velocity distributions were compared to determine the effects of the SiC particles on the in-flight velocities of the mixed feedstock powder particles. Significant differences between the particle velocities of the pure and the mixed feedstock powders might cause variations in the coating properties. The influence of the reinforcement phase within the coatings would then be difficult to dissociate from the one due to the particle velocities. Particle velocity measurements were performed using pure Al–12Si and a mixture of Al–12Si with 30% volume of SiC below 32 μm under the same operating conditions and the particle velocity distributions for these two feedstock powders are shown in Fig. 2. The velocities range from 300 to 900 m/s, with averages of 559 ± 132 m/s and

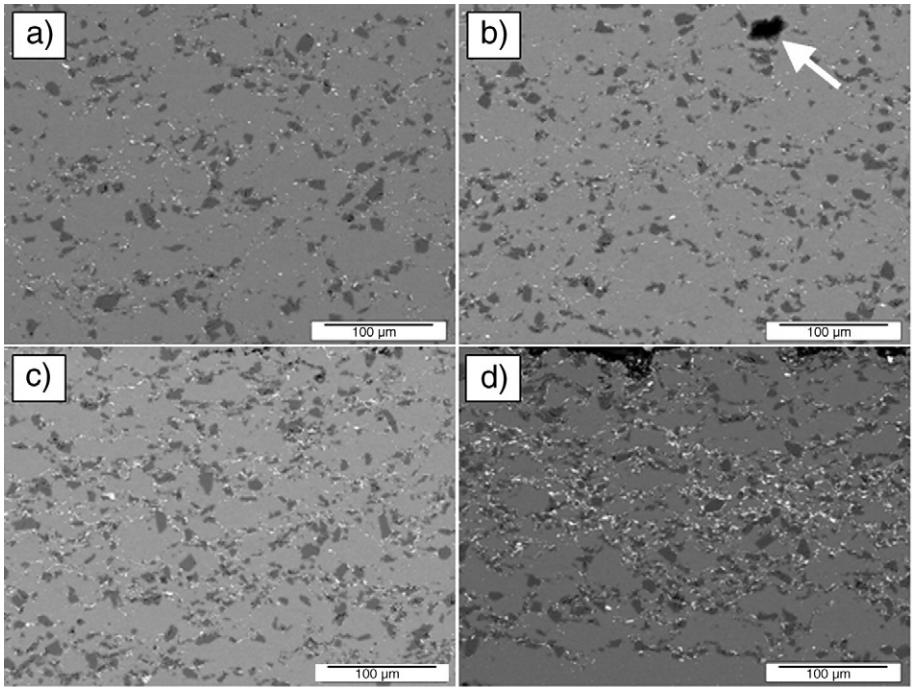

Fig. 3. SEM images of the cross-sections of composite coatings produced with feedstock powder containing Al–12Si and a) 20%, b) 30%, c) 40%, and d) 60% volume of SiC particles below 32 μm. The darker and white spots correspond to the SiC particles and spray gun material fragments within the aluminum matrix. The arrow points to a pore resulting from a SiC pullout.

581 ± 115 m/s for the pure and the mixed feedstock powders, respectively. Based on these results, it is concluded that adding 30% volume of SiC particles did not produce a significant change on the particle velocities. It is rationalized that the slight increase in the average velocity of the blended powders may be attributed to experimental errors. However, it is also possible that the SiC particles are accelerated to higher velocities than the Al–12Si particles which would in turn increase the average measured velocity. The SiC particles are of irregular shape and have a rougher surface which might increase both the drag coefficient and drag forces acting on the particles [33]. Since the reinforcement particles did not produce a significant change on the particle velocities, the variations in the coating properties, described in the following sections, will not be the result of a change in the particle velocity distribution but rather due to the presence of SiC particles in the mixed feedstock powders and coatings.

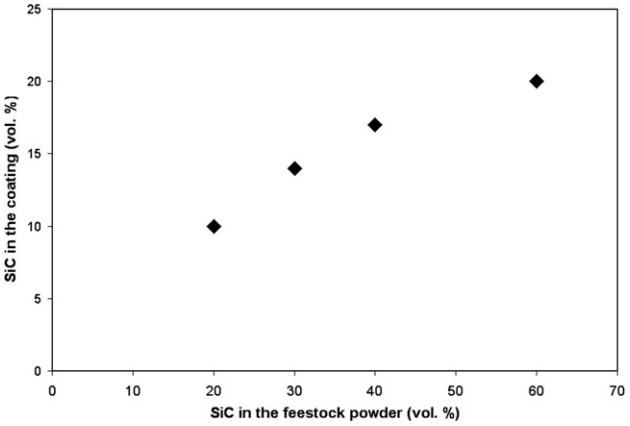

Fig. 5. Volume fraction of SiC in the coating as function of the SiC content in the feedstock powder.

3.2. Microstructure of the coatings

The SEM images of the cross-sections of CGDS coatings using mixed powders containing 20, 30, 40, and 60% volume of SiC are presented in Fig. 3. The coatings show a dense and clean microstructure and consist of deformed Al–12Si particles that surround the SiC particles. Porosity levels below 1% were found in all of the composite coatings. The interface between the particles of the matrix is difficult to detect as a result of significant plastic deformation upon impact. This suggests that the Al–12Si particles were accelerated beyond their critical velocity. The individual SiC particles, corresponding to the darker spots, are randomly distributed and homogeneously dispersed within the aluminum alloy matrix. Agglomerations of SiC particles, often experienced in casting and powder metallurgy of Al–SiC composites, were not observed in the coatings. The SiC particles in the coating maintained their angular morphology and the features of the initial feedstock powder (see Fig. 1b)), which demonstrates that upon impact, the SiC did not deform but became confined by the matrix material. A detailed analysis of the coatings images revealed that the average cross-sectional area of the individual SiC particles found in the coatings ranged from 20 to 30 μm^2 while the coating SiC volume content increased from 10 to 20%, respectively. This cross-sectional area of the individual SiC particles indicates that the reinforcement phase mostly consisted of fine particles. The inclusion of mostly small SiC particles in the coatings may be due to differences of the particle impact velocities between the smaller and the larger SiC particles. The momentum transfer between the gas and a particle, or the particle acceleration, is inversely proportional to the particle size. As a result, higher impact velocities are to be expected for the powders with a small size compared to the particles with a larger size. The small SiC particles would have struck the surface at higher velocities than the larger particles, deformed the aluminum matrix, and lodged themselves in the coatings. The larger SiC particles would not have caused a sufficiently large crater to stick in the coatings and therefore deflected off from the substrate.

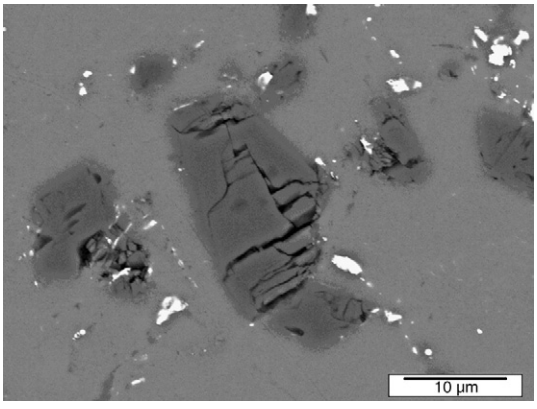

Fig. 4. SEM image at higher magnification of the central region of Fig. 3a) showing cracked SiC particles.

The isolated pore, indicated by the arrow in Fig. 3b) may have been the result of SiC pullouts during the polishing process. Pullouts have been observed in other studies on Al–SiC coatings [9,11]. The examination of Fig. 3a) at a higher magnification reveals the presence of fractured SiC particles (see Fig. 4). Different cutting blades were tested and the polishing techniques were varied to determine the effects of the metallographic procedures on these fissured SiC particles in the coatings. It was found that the defects detected in some of the SiC particles in the coatings were not influenced by the sample preparation methods. The breaking up of these SiC particles most likely occurred during the spraying process when SiC particles collided on the SiC particles in the coating. Such impacts could have extended the existing cracks or induced more defects in the SiC particles. It is expected that particles of Al–12Si striking the SiC would not have caused such fissures. These impacts would have been absorbed by the ductile matrix and have resulted in its plastic deformation around the hard reinforcement particles. Fracturing of reinforcement particles upon impact on the sprayed surface have also been reported during the production of MMC coatings by CGDS [32].

An electron-dispersive spectroscopy (EDS) analysis has revealed that the white regions observed in the coating images

were fragments of the spray gun material. This can easily be attributed to the presence of the silicon carbide particles, one of the hardest blasting media available, flowing through the nozzle. Those particles are likely to erode the walls of the spray gun during the spraying process and the wear debris are entrained and deposited with the composite feedstock powders. Moreover, increasing the SiC content of the feedstock powder accentuated the erosion of the walls of the spray gun. The coatings contained from 1 to 4% volume of wear debris as the SiC content in the feedstock powder was varied from 20 to 60% volume, respectively.

Composite coatings with SiC volume fractions varying from 10 to 20% have been produced from composite feedstock powders with SiC content of 20 to 60% volume respectively, as shown in Fig. 5. Upon impact on the sprayed surface, the SiC particles do not deform and a large fraction of particles bounce off from the surface. Some particles may implant themselves in the coating by deforming the matrix material upon hitting the surface. This is similar to surface grit contamination that occurs during the grit blasting process where blasting particles become embedded on the substrate surface. Grit residual content has been found to reach a maximum when the blasting angle is perpendicular to the surface to be cleaned [37,38] and increases with the blasting pressure [39,40]. In CGDS, the spray gun generally remains perpendicular to the substrate in order to maximize the deposition efficiency [41] and the operating pressure is well above the ones used in grit blasting. It is also believed that since the constituents of the feedstock powder hit the substrate simultaneously, the Al–12Si particles can deform around the SiC particles and entrap these reinforcements in the coating.

The fraction of SiC retained in the coatings was found to decrease as the SiC volume fraction in the feedstock powders increased, as illustrated in Fig. 6. For example, in coatings produced with feedstock powders containing 20 and 60% volume of SiC, 50 and 33% of the SiC were preserved, respectively. Increasing the fraction of SiC in the feedstock powder augments the number of impacts of SiC particles on the sprayed surface. Some of these SiC particles will be entrapped in the coating while others will bounce off the surface. However, fewer particles of Al–12Si can deform around the embedded SiC particles which reduces the proportion of SiC retained in the coating. In order to entrap as much SiC particles as possible, there must be sufficient matrix material to contain the reinforcement particles in the coating.

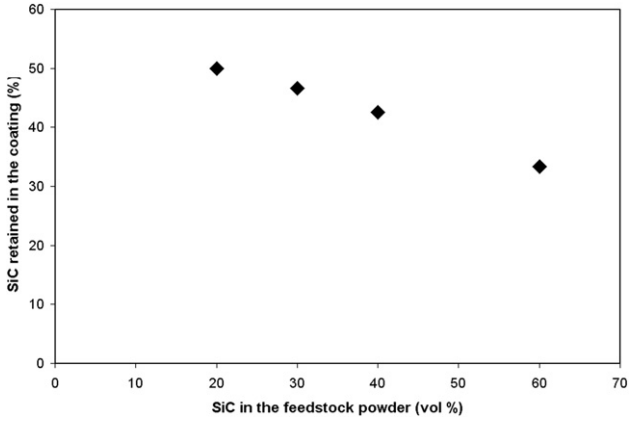

Fig. 6. Fraction of SiC retained in the coatings as a function of the SiC content in the feedstock powder.

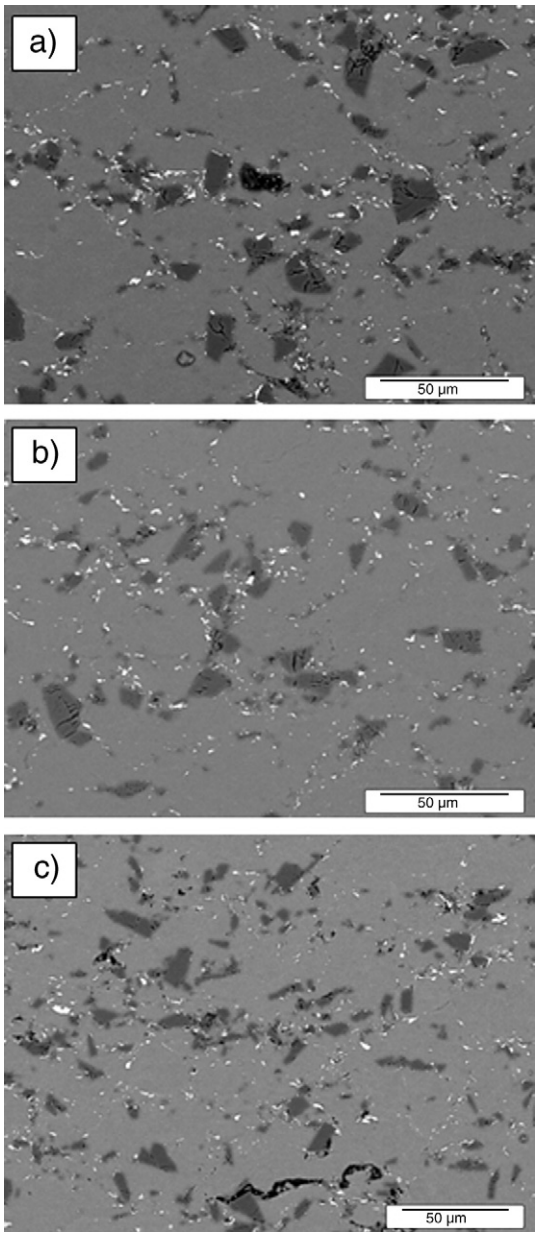

Fig. 7. SEM images of the cross-sections of composite coatings produced with feedstock powder containing Al–12Si and 20% volume of SiC particles below a) 25 μm, b) 32 μm, and c) 38 μm.

The SEM images of the coatings produced with feedstock powder containing 20% volume of SiC particles sieved below 25, 32, and 38 μm, are shown in Fig. 7. Close examination of this figure reveals that the size range of the SiC particles in the feedstock powder used in this study did not influence the overall microstructure of the coating. In every coating shown, the SiC particles are randomly distributed within the Al–12Si matrix, while

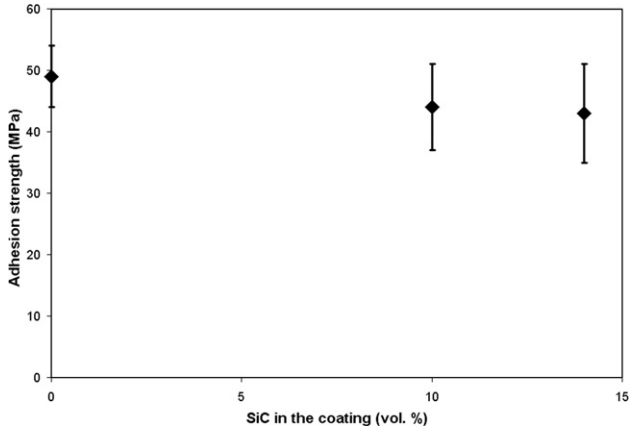

Fig. 8. Adhesion strength of SiC-reinforced Al–12Si coatings as a function of the SiC content in the coating.

containing 10% volume of SiC and exhibiting a porosity below 1%. The average cross-sectional area of the individual SiC particles in the coatings produced with SiC particles sieved below 25, 32, and 38 μm were 20, 20, and 40 μm^2, respectively. Although larger SiC particles were included in the feedstock powder, the reinforcement phase of the coating consisted of fine SiC particles, as it can be observed in Fig. 7. This is attributed to the high particle velocities associated to the small SiC particles. These particles stuck to the sprayed surface by causing deformation of the matrix material on impact. Because of their lower velocities, the larger SiC particles did not sufficiently deform the sprayed surface. During the spraying process, these particles deflected off the surface on impact and were not retained in the coating.

The retained fraction of SiC in the current work is different than what was reported in another study, where 40% volume of the SiC was retained in the coatings regardless of the SiC content in the feedstock powder [28]. In that study, aluminum particles with a diameter ranging from 51 to 63 μm were used and the particle velocities varied from 400 to 500 m/s. These differences in the particle size and velocities may have influenced the amount of SiC that could be contained in the coatings.

The loss of SiC particles during the spraying process is unavoidable when blends of aluminum alloy powder and SiC particles are used. In CGDS, the particles must be accelerated above a critical velocity to plastically deform, bond to the substrate, and build up the coating. However, since SiC is a brittle material, its particles did not deform on impact on the substrate.

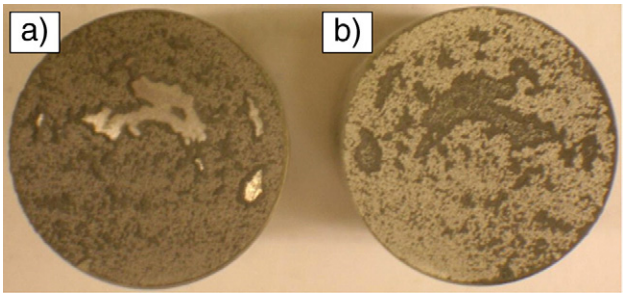

Fig. 9. Photograph of the bond strength specimens with a) the bonding agent and b) the remainder of the pure Al–12Si coating after the bond test.

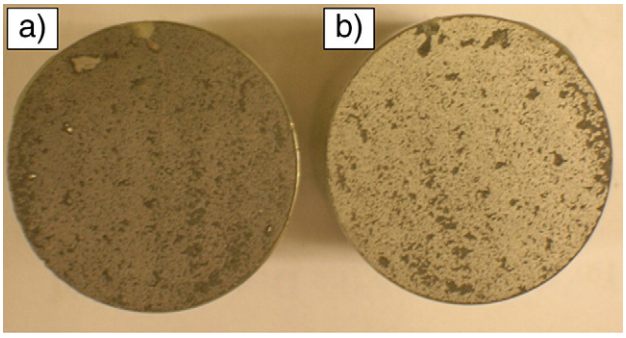

Fig. 10. Photograph of the bond strength specimens with a) the bonding agent and b) the remainder of the Al–12Si coating with a SiC content of 14% volume after the bond test.

SiC particles become embedded on the sprayed surface and are entrapped by Al–12Si particles that deform around the SiC particles. Reinforcement particles with a fine size distribution could improve the fraction of SiC retained in the coating. The small particles would impact on the sprayed surface at high velocities and become embedded in the coating. Composite powder particles produced by mechanically milling and alloying aluminum and SiC particles may also minimize these losses. As it was described earlier, the mechanical alloying process produces agglomerations of aluminum particles with entrapped fragments of SiC and the resulting composite particles have fine and uniformly distributed reinforcements in the matrix [9,11,14]. In plasma spraying, milled powders improve the wettability of SiC by aluminum and augment the fraction of SiC retained in the coatings. However, in CGDS, such composite particles may not undergo the same level of plastic deformation observed in Al–12Si particles. The reinforcements in the composite powder particles might obstruct and limit the deformation of the matrix, which would lead to higher porosity levels in the coating [25].

3.3. Bond strength measurements

The variation of the coating adhesion strength as a function of the SiC content in the coating is shown in Fig. 8. Adhesion strength values of 49 ± 5, 44 ± 7, and 43 ± 8 MPa were obtained as the volume fraction of SiC in the coatings increased from 0, 10, and 14%, respectively. Examination of the specimens revealed that the failure occurred at the coating–substrate interface. Most of the coatings remained attached to the specimens on which the bonding agent was applied, as shown in Figs. 9 and 10. An increase of the SiC content in the coating slightly reduced the level of adhesion of the coatings on the substrates. Although the SEM images of the SiC-reinforced coatings revealed substrate–coatings interfaces free of defects that could alter the adherence of the coating, the presence of SiC particles at the interface may have affected the adhesion strength (see Fig. 11). These SiC particles reduced the surface area available for the aluminum matrix to deform around the surface irregularities of the substrate and bond to the latter. As more SiC particles impinged on the substrate, fewer aluminum alloy particles came in contact with the substrate. The number of anchoring sites between the coating and the substrate are then

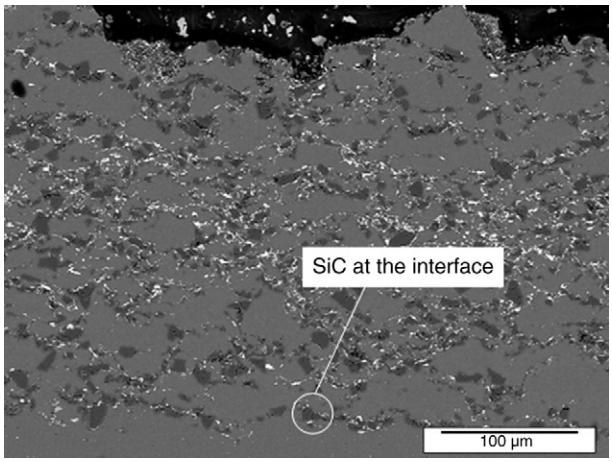

Fig. 11. SEM image of the substrate–coating interface of a composite coating containing 20% volume of SiC.

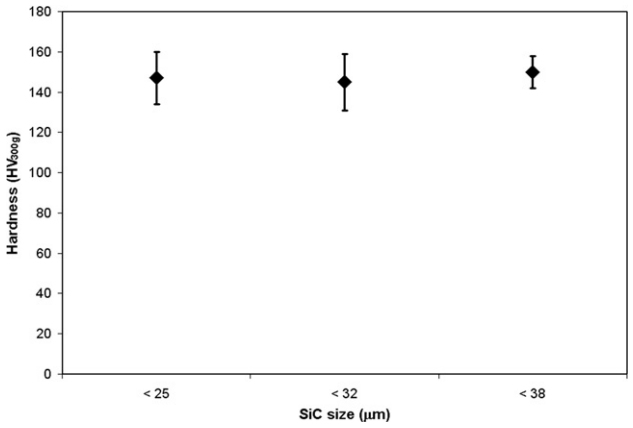

Fig. 13. Hardness of SiC-reinforced Al–12Si coatings produced with feedstock powder containing 20% volume of SiC particles of different size distributions. Each coating contained 10% volume of SiC.

reduced in comparison to coatings reinforced with a lower SiC volume fraction. A thin coating layer of pure Al–12Si could then be sprayed on the surface of the substrate before spraying mixed feedstock powders to reduce the effects of the SiC particles at the substrate–coating interface. The adhesion strength of Al–SiC coatings produced by plasma spraying was found to vary from 68 MPa to 76 MPa due to the formation of a metallurgical bond between the coating and the substrate [9]. In addition, it was reported that a decrease in the metal content at the interface also reduced the strength of the bond. The reported bond strength values in this study are below the ones in coatings produced by plasma spraying because of the nature of the bond. In CGDS, the bonding mechanism is through mechanical anchoring since no bulk particle melting occurs and no metallurgical reactions take place between the sprayed material and the substrate [24].

3.4. Hardness measurements

The SiC particles in the coatings initiated significant changes in the coating hardness, as illustrated in Fig. 12. The average hardness of Al–12Si reinforced with SiC particles varied form 145±14 to 205±25 $HV_{300\ g}$ for coatings containing 10% to 20% volume of SiC. A hardness of 110±25 $HV_{300\ g}$ was obtained for an Al–12Si coating without SiC reinforcements. Thus, coatings with 10% volume of SiC were found to be 32% harder than pure Al–12Si coatings. The microhardness values of the coatings produced with feedstock powders containing 20% volume of SiC particles below 25, 32, and 38 µm are given in Fig. 13. The coating hardness values were not altered by the size of the SiC particles in the feedstock powders. As it was shown in Fig. 7, the reinforcement phase in the coatings consisted of fine SiC particles even though the SiC particle size distribution in the feedstock powders was varied.

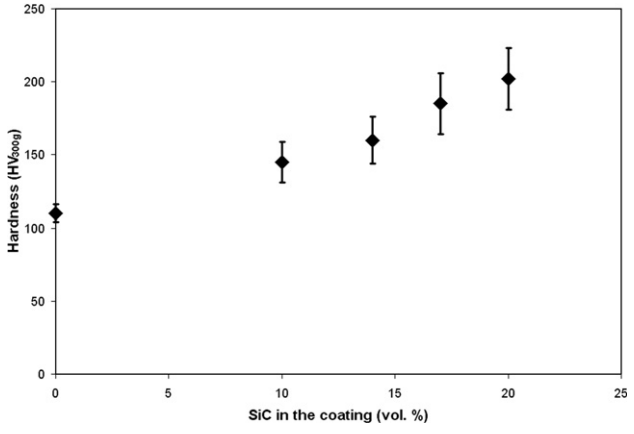

Fig. 12. Hardness of SiC-reinforced Al–12Si coatings as a function of the SiC content in the coatings.

4. Conclusions

SiC-reinforced Al–12Si alloy coatings were successfully produced by the CGDS process. The microstructures of the composite coatings were examined to obtain the retained fraction of the SiC reinforcements and the porosity. The results showed that between 33% and 50% of the SiC blended with the aluminum matrix was embedded in the composite coatings. The coatings exhibited porosity levels below 1%. The SiC particles exhibited a reasonably uniform distribution within the aluminum matrix and significantly improved the coating hardness. A hardness values ranging from 145 to 205 $HV_{300\ g}$ were obtained for Al–12Si coating reinforced with SiC contents varying from 10 to 20% volume. These represent a 32 and 86% rise in hardness, respectively, when compared to pure Al–12Si coatings. It was also found that the size of the reinforcement phase embedded in the coatings consisted of fine SiC particles. A fine size distribution of the SiC particles may improve the fraction of SiC retained in the coatings. Bond strength tests demonstrated that the adhesion strength of the coatings to their substrate slightly decreased as the SiC content increased. The presence of SiC particles at the substrate–coating interface reduces the number of anchoring sites between the coating and the substrate. Particle velocity measurements of pure and mixed feedstock powders confirmed that the variations in the mechanical properties of the coatings were not the result of a change in the particle velocity but rather due to the

presence of SiC particles in the mixed feedstock powders and coatings.

Acknowledgements

The authors wish to acknowledge the financial support of the Natural Sciences and Engineering Research Council of Canada (NSERC) as well as the Centre québécois de recherche et de développement de l'aluminium (CQRDA). They also thank Dr. Mathieu Brochu of McGill University for his help with the SEM samples preparation and characterization. The assistance of Chrystelle Thibault Boyer with the powder preparation and with the coating production is appreciated.

References

[1] S.C. Tjong, Z.Y. Ma, Mater. Sci. Eng., R 29 (2000) 49.
[2] D.B. Miracle, Compos. Sci. Technol. 65 (2000) 2526.
[3] Ü. Cöcen, K. Önel, Compos. Sci. Technol. 62 (2002) 275.
[4] S.C. Tjong, S.Q. Wu, H.C. Liao, Compos. Sci. Technol. 57 (1997) 1551.
[5] A. Pardo, M.C. Merino, J. Rams, S. Merino, F. Viejo, M. Campo, Oxid. Met. 63 (2005) 215.
[6] T.F. Klimowicz, J. Met. 46 (11) (1994) 49.
[7] D.M. Schuster, M.D. Skibo, R.S. Bruski, R. Provencher, G. Riverin, J. Met. 45 (5) (1993) 26.
[8] T.P.D. Rajan, R.M. Pillai, B.C. Pai, J. Mater. Sci. 33 (1998) 3491.
[9] K. Ghosh, T. Troczynski, A.C.D. Chaklader, J. Therm. Spray Technol. 7 (1) (1998) 78.
[10] B. Torres, M. Campo, A. Ureña, J. Rams, Surf. Coat. Technol. 201 (2007) 7552.
[11] M. Gui, S.B. Kang, K. Euh, J. Therm. Spray Technol. 13 (2) (2004) 214.
[12] M. Gui, S.B. Kang, Mater. Lett. 46 (2000) 296.
[13] M. Gui, S.B. Kang, Mater. Lett. 51 (2001) 396.
[14] K.A. Khor, F.Y.C. Boey, Y. Murakoshi, T. Sano, J. Therm. Spray Technol. 3 (2) (1994) 162.
[15] T. Itsukaichi, T.W. Eagar, M. Umemoto, I. Okane, Weld. Res. Supplement (1996) 285-s.
[16] A.P. Alkhimov, V.F. Kosarev, A.N. Papyrin, Sov. Phys. Dokl. 35 (1990) 1047.
[17] A.P. Alkhimov, A.N. Papyrin, V.F. Kosarev, US Patent 5 302 414 (1994).
[18] T.H. Van Steenkiste, J.R. Smith, J. Therm. Spray Technol. 13 (2) (2004) 274.
[19] V. Shukla, G.S. Elliot, B.H. Kear, J. Therm. Spray Technol. 9 (3) (2000) 394.
[20] R.S. Lima, J. Karthikeyan, C.M. Kay, J. Lindermann, C.C. Berndt, Thin Solid Films 416 (2002) 129.
[21] L. Ajdelsztajn, B. Jodoin, G.E. Kim, J.M. Schoenung, Met. Mater. Trans. A 36 (2005) 657.
[22] L. Ajdelsztajn, E.J. Lavernia, B. Jodoin, P. Richer, E. Sansoucy, J. Therm. Spray Technol. 15 (4) (2006) 495.
[23] S. Yoon, H.J. Kim, C. Lee, Surf. Coat. Technol. 200 (2006) 6022.
[24] R.C. Dykhuizen, M.F. Smith, J. Therm. Spray Technol. 7 (2) (1998) 205.
[25] E. Sansoucy, B. Jodoin, P. Richer, L. Ajdelsztajn, Int. Therm. Spray Conf. 2006 Proceedings, Seattle, WA, USA, May 2006.
[26] L. Ajdelsztajn, A. Zúñiga, B. Jodoin, E.J. Lavernia, J. Therm. Spray Technol. 15 (2) (2006) 184.
[27] L. Zhao, K. Bobzin, D. He, J. Zwick, F. Ernst, E. Lugscheider, Adv. Eng. Mater. 8 (4) (2006) 264.
[28] G.L. Eesly, A. Elmoursi, N. Patel, J. Mater. Res. 18 (4) (2003) 855.
[29] T.H. Van Steenkiste, A. Elmoursi, D. Gorkiewicz, B. Gillispie, Surf. Coat. Technol. 194 (2005) 103.
[30] H.Y. Lee, Y.H. Yu, Y.C. Lee, Y.P. Hong, K.H. Ko, J. Therm. Spray Technol. 13 (2) (2004) 184.
[31] Z.B. Zhao, B.A. Gillispie, J.R. Smith, Surf. Coat. Technol. 200 (2006) 4746.
[32] J. Haynes, A. Pandey, J. Karthikeyan, A. Kay, Int. Therm. Spray Conf. 2006 Proceedings, Seattle, WA, USA, May 2006.
[33] B. Jodoin, L. Ajdelsztajn, E. Sansoucy, A. Zúñiga, P. Richer, E.J. Lavernia, Surf. Coat. Technol. 201 (2006) 3422.
[34] Clemex Vision 5.0 User guide (2007).
[35] ASTM C 633-01, "Standard Test Method for Adhesion or Cohesion Strength of Thermal Spray Coatings," ASTM International.
[36] DPV-2000 — Reference Manual Rev. 5.0, Tecnar Automation, 45 pages.
[37] M. Mellali, A. Grimaud, A.C. Leger, P. Fauchais, J. Lu, J. Therm. Spray Technol. 6 (2) (1997) 217.
[38] J. Day, X. Huang, N.L. Richards, J. Therm. Spray Technol. 14 (4) (2005) 471.
[39] S. Amada, T. Hirose, T. Senda, Surf. Coat. Technol. 111 (1999) 1.
[40] M.F. Bahdou, P. Nylen, J. Wigren, J. Therm. Spray Technol. 13 (4) (2004) 508.
[41] D.L. Gilmore, R.C. Dyknuizen, R.A. Neiser, T.J. Roemer, M.F. Smith, J. Therm. Spray Technol. 8 (4) (1999) 576.